# Supporting Information

## Efficient synthesis of furfuryl alcohol from $H_2$-hydrogenation/transfer hydrogenation of furfural using sulfonate group modified Cu catalyst

*Wanbing Gong,[†,‡] Chun Chen,*[†] Yong Zhang,[†,‡] Hongjian Zhou,[†] Huimin Wang,[†] Haimin Zhang,[†] Yunxia Zhang,[†] Guozhong Wang[†] and Huijun Zhao*[*,†,§]*

[†] Key Laboratory of Materials Physics, Centre for Environmental and Energy Nanomaterials, Anhui Key Laboratory of Nanomaterials and Nanotechnology, Institute of Solid State Physics, Chinese Academy of Sciences, Hefei 230031, P. R. China

[‡] University of Science and Technology of China, Hefei, Anhui 230026, P. R. China

[§] Centre for Clean Environment and Energy, Gold Coast Campus, Griffith University, Queensland 4222, Australia

*Corresponding Author. Email: h.zhao@griffith.edu.au, chenchun2013@issp.ac.cn

## 1 Experimental Section

### 1.1 $H_2$-TPR and $N_2O$ titration

$H_2$-TPR and $N_2O$ titration were performed on the Chemisorb 2720 instrument (Micromeritics, USA) equipped with a thermal conductivity detector (TCD). First, 50 mg of catalyst was purged with He (30 mL/min) at 300 °C for 1 h. After being cooled to 40 °C, the calcined catalyst was reduced in a 5 vol % $H_2$/Ar mixture (40 mL/min) to a final temperature of 350 °C with a heating rate of 10 °C/min. The amount of $H_2$ consumption was denoted as $A_1$. Second, $N_2O$ (30 mL/min) was used to oxidize the surface Cu to $Cu_2O$ at 30 °C for 0.5 h. Subsequently, the catalyst was purged with He (30 mL/min) at 30 °C for 0.5 h to remove residual $N_2O$. Finally, the oxidized catalyst was reduced in a 5 vol % $H_2$/Ar mixture (40 mL/min) to a final temperature of 350 °C with a heating rate of 10 °C/min. The amount of $H_2$ consumption was denoted as $A_2$. The dispersion (D) of Cu was calculated as follows: $D = 2A_2/A_1 \times 100\%$. The specific area of Cu was calculated from the amount of $H_2$ consumption ($A_2$) with $1.46 \times 10^{19}$ copper atoms/$m^2$. The average diameter can be calculated as follows: $d = 6/(S \times \rho_{Cu}) \approx 0.5 \times A_1/A_2$ (nm). $\rho_{Cu}$ in this equation is the density of copper (8.92 g/$cm^3$).

### 1.2 $N_2$ physisorption technique

Specific surface area ($S_{BET}$) and pore volume ($V_{pore}$) of samples were determined by $N_2$ physisorption technique. The BET surface area was calculated using the Brunauer-Emmett-Teller equation. The pore volume was calculated from the desorption branches of the nitrogen isotherms employing the Barrett-Joyner-Halenda (BJH) model.

## 2 Characterizations of Catalysts

### 2.1 The TEM images of Cu catalysts

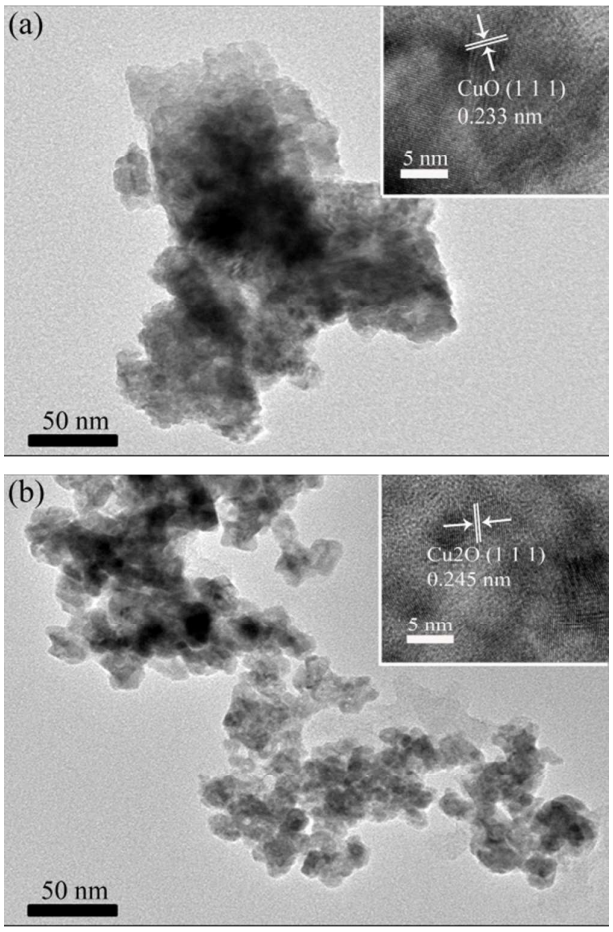


**Figure S1.** TEM images of (a) Cu/AC and (b) Cu/AC-$SO_3H$ (Insert is HRTEM images of (a) Cu/AC and (b) Cu/AC-$SO_3H$).

The pictures of Cu/AC and Cu/AC-$SO_3H$ catalyst were shown in Figure S1. Due to homogeneous distribution and small size of metallic particles, the morphology and size distribution of Cu nanoparticles could not be easily discerned in the TEM images, which may be affected by this preparation method. However, from the pictures, it was

evidently found Cu/AC-$SO_3H$ had a better dispersion and smaller size of metallic particles than Cu/AC catalyst which showed a relatively obvious aggregation of metallic particles. The -$SO_3H$ group on the surface of support in Cu/AC-$SO_3H$ could act as nanoparticle stabilizers and dispersants, thus, limiting their growth and aggregation. HRTEM images of the two kinds of Cu catalyst had also been used to indicate crystalline nature of nanocrystals, as shown in the insert pictures. Noticing that the Cu/AC and Cu/AC-$SO_3H$ catalysts were both prepared in liquid phase reduction method without sintering and reduction at high temperature, the two kinds of catalysts showed weak crystallization. The lattice distances of the selected area for Cu/AC and Cu/AC-$SO_3H$ catalysts were calculated to be 0.233 nm and 0.245 nm, which matched with the (111) planes of CuO and (111) plane of $Cu_2O$, respectively.

## 2.2 **Characterization of Catalysts (XPS)**

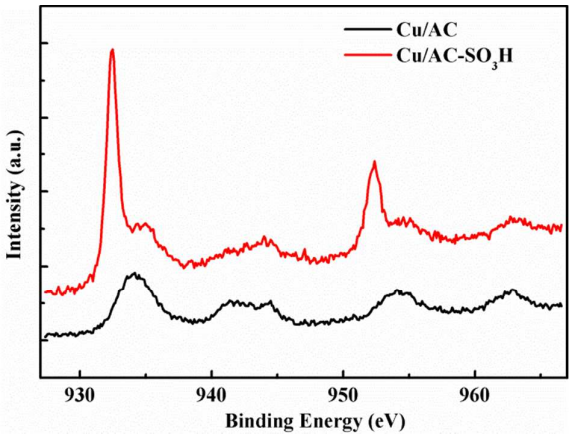


Figure S2. The XPS spectra of Cu/AC and Cu/AC-$SO_3H$.

Figure S2 is the XPS spectra of Cu/AC and Cu/AC-$SO_3H$. Two broader shake-off bands at 940-945 and 960-965 eV, which is related to Cu(II), are observed in the two samples.

## 2.3 Characterization of Catalysts (BET)

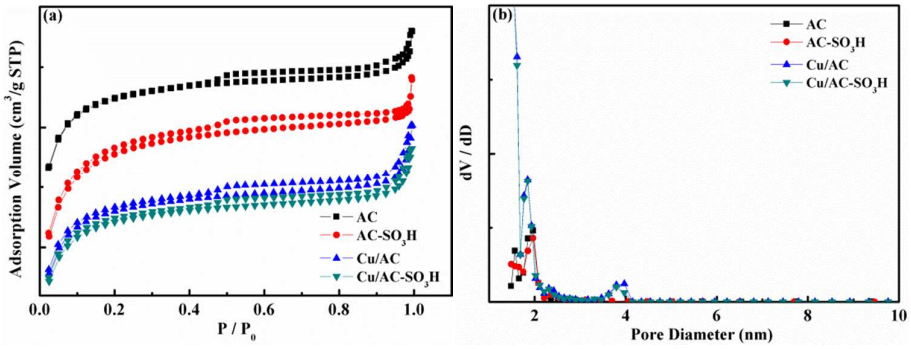


**Figure S3.** (a) $N_2$ sorption isotherms and (b) BJH pore size distribution plots.

It was found that all of samples were microporous solids with a little contribution of mesopores from the Figure S3.

**3 Results**

3.1 Catalytic performance over different catalysts

**Table S1.** Catalytic performance over different catalysts for FAL hydrogenation[a]

| Catalysts | Temperature (K) | FAL conversion (%) | Product selectivity (%) FOL | THFOL | Others |
|---|---|---|---|---|---|
| Cu/AC-$SO_3H$ | 373 | >99.9 | >99.9 | -- | -- |
| AC | 373 | -- | -- | -- | -- |
| AC-$SO_3H$ | 373 | -- | -- | -- | -- |
| Pd/AC-$SO_3H$ | 313 | >99.9 | 5.7 | 52.4 | 41.9 |
| Pd/AC-$SO_3H$ | 373 | >99.9 | 7.8 | 73.1 | 19.1 |
| Cu/AC + $H_2SO_4$ | 373 | 25.6 | -- | -- | >99.9 |

[a] Reaction conditions: catalyst to FAL mass ratio = 1:1; FAL = 1.0 mmol; $H_2$ pressure = 1.0 MPa; 2-propanol = 5 mL; reaction time = 3.0 h.

We investigate and compare the Cu/AC-$SO_3H$ catalyst with AC, AC-$SO_3H$, Pd/AC-$SO_3H$ and Cu/AC+$H_2SO4$ catalysts on the furfural hydrogenation using 2-propanol as solvent. For the catalyst without active metal (AC and AC-$SO_3H$), there is no activity on furfural hydrogenation and etherification of the furfural with 2-propanol. When using dilute sulfuric acid + Cu/AC as catalyst, a certain degree of etherification has been observed. This result indicates the acidity of AC-$SO_3H$ is insufficient as an acid site for etherification of furfural with solvent. On the other hand, unlike Cu/AC-$SO_3H$ catalyst, both of hydrogenation and esterification of furfural have been observed over the Pd/AC-$SO_3H$ catalyst indicating the active metal can also influences the product distribution on furfural hydrogenation. In addition, the

interaction between furfural and solvent is weakened at a higher reaction temperature, like the reaction condition used in our work.

### 3.2 Calculation of TOF and Activation Energy

The turnover frequency (TOF) was calculated to investigate the intrinsic catalytic activity, which was defined as the moles of converted FAL made per catalytic site and per unit time. In this paper, TOF was calculated in a low activity. And the initial FAL hydrogenation rate (r) was expressed by g of catalyst (mol $g^{-1}$ $h^{-1}$).[1] The results, presenting in Table S2, showed that the initial catalytic activity increase with reaction temperature. The higher initial catalytic performance of Cu/AC-$SO_3H$ could also be seen in this table. Arrhenius-type plots are presented in Figure S4. The apparent activation energy (*Ea*) was determined to be 131 and 189 kJ/mol for the Cu/AC-$SO_3H$ and Cu/AC catalysts, respectively.

**Table S2.** Catalytic performance of Cu-based catalysts in FAL hydrogenation[a]

| Run. no. | Temperature (K) | FOL yield (%) | TOF[b] ($h^{-1}$) | r[c] (mol $g^{-1}_{Cu}$ $h^{-1}$) |
|---|---|---|---|---|
| Cu/AC: | | | | |
| 1 | 368 | -- | -- | -- |
| 2 | 383 | -- | -- | -- |
| 3 | 393 | -- | -- | -- |
| 4 | 403 | 2.4 | 0.428 | 0.0004 |
| 5 | 408 | 6.8 | 1.239 | 0.0012 |
| 6 | 413 | 20.6 | 3.779 | 0.0038 |
| 7 | 418 | 29.6 | 5.431 | 0.0055 |
| 8 | 423 | 46.8 | 8.583 | 0.0088 |

| | | | | |
|---|---|---|---|---|
| 9 | 428 | 72.5 | 13.295 | 0.0136 |
| Cu/AC-$SO_3H$: | | | | |
| 1 | 368 | 3.6 | 0.799 | 0.0019 |
| 2 | 373 | 6.5 | 1.443 | 0.0034 |
| 3 | 378 | 8.2 | 1.826 | 0.0044 |
| 4 | 383 | 24.4 | 5.431 | 0.0131 |
| 5 | 388 | 36.8 | 8.177 | 0.0198 |
| 6 | 393 | 51.1 | 11.355 | 0.0274 |

[a] Reaction conditions: catalyst to FAL mass ratio = 1:1; FAL = 1.0 mmol; $H_2$ pressure = 0.4 MPa; 2-propanol = 5 mL; reaction time = 3.0 h (Cu/AC), 1.0 h (Cu/AC-$SO_3H$).

[b] Turnover frequency (TOF) = $mol_{FAL}/(mol_{exposed\ surface\ Cu} \cdot h)$.

[c] Initial conversion rate of FAL.

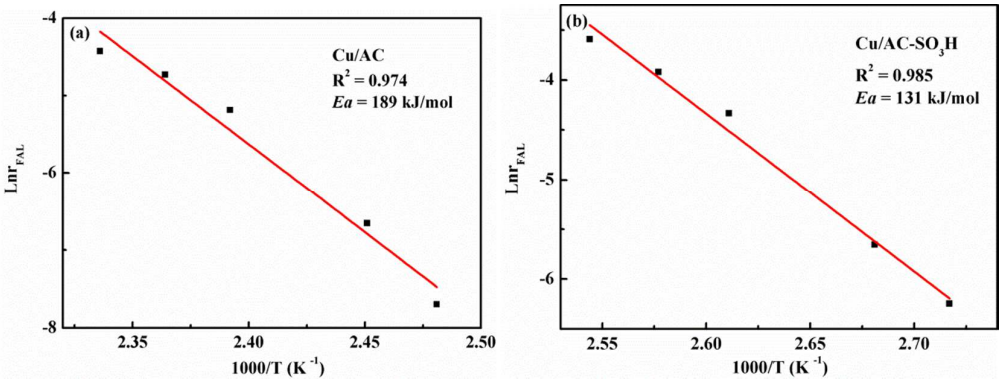


**Figure S4.** Arrhenius type plots of catalytic activity for the hydrogenation of FAL over the Cu/AC and Cu/AC-$SO_3H$.

### 3.3 Molecular Dynamics Simulation for adsorption of furfural (FAL) and Cu-based catalyst

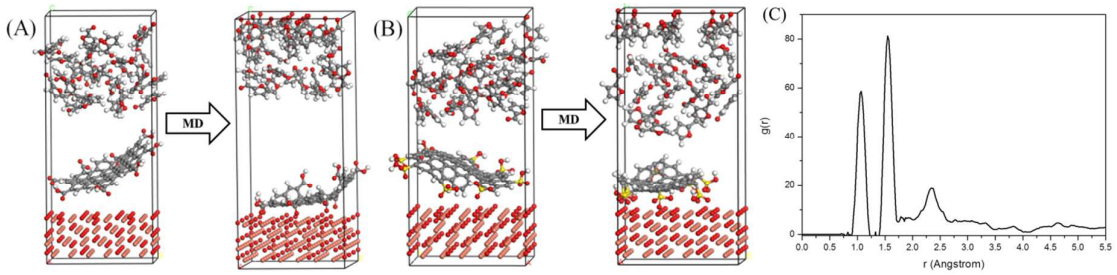


**Figure S5**. Snapshots of CGF (A) and CSGF (B) model before (left) and after (right) MD simulation. Color codes: Cu atom, jacinth; carbon atom, gray; hydrogen atom, white and oxygen atom, red; sulfur atom, yellow. (C) The radial distribution function of CSGF model.

**Table S3.** Interaction energies between FAL and $Cu_2O$

| Surface | Organism | $E_{total}$ (kcal·mol$^{-1}$) | $E_{Cu2O}$ (kcal·mol$^{-1}$) | $E_{furfural}$ (kcal·mol$^{-1}$) | $E_{interaction}$ (kcal·mol$^{-1}$) |
|---|---|---|---|---|---|
| $Cu_2O$ (111) | non-sulfonated | $1.9903\times10^5$ | 455.306 | $2.0198\times10^5$ | -6192.284 |
| $Cu_2O$ (111) | sulfonated | $1.9839\times10^5$ | 203.361 | $2.0197\times10^5$ | -7058.543 |

Molecular dynamics (MD) simulation was adopted to simulate the adsorption of FAL on two types of Cu-based catalysts, Cu/AC-$SO_3H$ and Cu/AC. The MD simulation was conducted with Material Studio (MS) v4.2 packages (Accelrys, San Diego, CA) using condensed-phase optimized molecule potentials for atomistic simulation studies (COMPASS) force field. Based on the experimental condition, we designed (i) $Cu_2O$/graphene/FAL (CGF) model; (ii) $Cu_2O$/sulfonated graphene/FAL (CSGF)

model, respectively. Here, graphene was used to replace AC due to no AC model in the system. Accroding to the calculation, it was found the texture of support, graphene or AC, would not obviously influence the simulation process. Adhesion between $Cu_2O$ and FAL molecules could be evaluated by the interaction energy between $Cu_2O$ crystallographic surfaces and FAL molecules. Interaction energies between $Cu_2O$ and FAL were calculated by COMPASS force field and the results are listed in Table S3. From results of the simulation, the interaction energies of all systems were negative values, clearly indicating that the FAL molecules were easily combined with the surface of the $Cu_2O$ crystal. Moreover, compared with the two models, the interaction energy of the CSGF model was the higher than the CGF model, which indicated that the stronger interaction existed between FAL and the sulfonated $Cu_2O$ (111) surface. Moreover, this result showed that the sulfonated functional group is favorable to improve the catalytic activity of $Cu_2O$ NPs. Results of MD simulation provided strong evidence to explain the related catalytic reaction of FAL by sulfonated modification, which was in good agreement with those from both experiments and MD simulations. In the CSGF model, the highest peak appears at 1.55 Å; meanwhile, there are also peaks occurring at 1.07 Å and 2.35 Å (Figure S5(C)). Therefore, this result indicated that the adsorption of FAL on the sulfonated $Cu_2O$ nano-catalyst is related to hydrogen bond.

### 3.4 Hydrogenation of FAL over reduced Cu catalysts

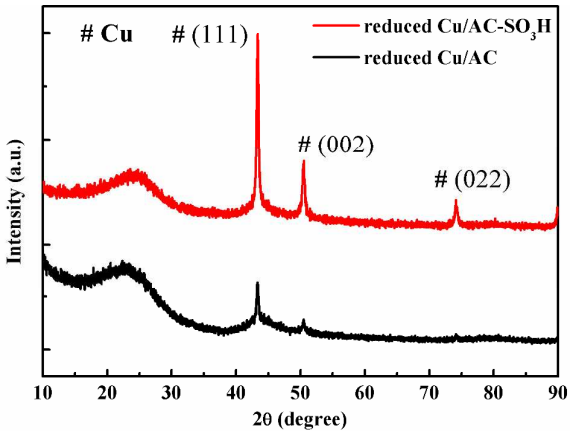


**Figure S6.** The XRD patterns of reduced Cu/AC and Cu/AC-$SO_3H$ catalysts.

**Table S4.** Catalytic performance for FAL hydrogenation over reduced Cu/AC and Cu/AC-$SO_3H$[a].

| Catalysts | FOL yield (%) |
|---|---|
| Cu/AC | <0.1 |
| Cu/AC-$SO_3H$ | >99.9 |
| reduced Cu/AC | 5.6 |
| reduced Cu/AC-$SO_3H$ | 13.2 |

[a] Reaction conditions: catalyst to FAL mass ratio = 1:1; FAL = 1.0 mmol; reaction temperature = 383 K, time = 120 min, $H_2$ pressure = 0.4 MPa, 2-propanol = 5 mL.

### 3.5 Comparing with references

**Table S5.** Summary of heterogeneous catalysts for hydrogenation of FAL to FOL in recent published works

| Catalysts | Reaction conditions[a] | | | FOL Yield | Cycle tests |
|---|---|---|---|---|---|
| | T(K) | $P_{H2}$(MPa) | t(h) | (%) | |
| 5 % Pd-5%Cu/MgO[2] | 383 | 0.6 | 1.33 | 98.6 | 1st to 5th (unchanged) |
| 15 wt% Cu/ SBA-15[3] | 443 | -- | 5.0 | 51.9 | -- |
| Cu(40%)–Mg–Al[4] | 423 | 0.0 | 6.0 | 100.0 | -- |
| CuMgAl[1] | 383 | 1.0 | 4.0 | 100.0 | -- |
| Cu–MgO[5] | 453 | 0.1 | -- | 96.0 | -- |
| $Cu/Fe_2O_3$[6] | 453 | 0.0 | 7.5 | 28.0 | -- |
| $Cu/SiO_2$[7] | 413 | 0.1 | -- | 62.1 | -- |
| Cu/HT[8] | 423 | 3.0 | 8.0 | 89.0 | -- |
| Cu:Zn:Cr:Zr (3:2:1:3)[9] | 443 | 2.0 | 3.5 | 96.0 | 1st to 5th (slight decrease) |
| Co–Cu/SBA-15[10] | 443 | 2.0 | 4.0 | 80.0 | 1st to 3th (slight decrease) |
| Co–Cu/SBA-15[11] | 403 | 3.0 | 3.0 | 96.7 | -- |
| $Pt–Sn/SiO_2$[12] | 373 | 1.0 | 4.0 | 96.0 | -- |
| This work | 378 | 0.4 | 2.0 | >99.9 | 1st to 5th (slight decrease) |
| This work | 423 | 0.0 | 5.0 | >99.9 | -- |

[a] $P_{H2}$ = 0.0 MPa: transfer hydrogenation; $P_{H2}$ > 0.0 MPa; hydrogenation by $H_2$.

As summarized in Supplementary Table S5, it was noticed that most of the reported

catalysts for hydrogenation of FAL to FOL were supported Cu catalysts. Compared with the reported Cu based catalysts, the prepared Cu/AC-$SO_3H$ catalyst exhibited the exceptionally high yield (> 99.9 %) in the mildest reaction condition when applied in hydrogenation of FAL to FOL, even better than some of supported noble catalysts. Another prominent advantage of this catalyst is their reusability. The Cu/AC-$SO_3H$ catalyst showed nearly stable activity for five recycles in liquid phase FAL hydrogenation to FOL.

### 3.6 Hydrogenation of FAL over Cu/AC-$SO_3H$ during the heating stage

**Table S6.** Hydrogenation of FAL over Cu/AC-$SO_3H$ during the heating stage [a]

| Run. no. | Heating stage (K) | $H_2$ pressure (MPa) | Time (min) | FOL yield (%) |
|---|---|---|---|---|
| 1 | 298-318 | 0.4 | 10.0 | 0.0 |
| 2 | 318-338 | 0.4 | 20.0 | 0.0 |
| 3 | 338-378 | 0.4 | 40.0 | 2.4 |

[a] Reaction conditions: catalyst to FAL mass ratio = 1:1; FAL = 1.0 mmol; 2-propanol = 5 mL.

In order to test the performance of FAL hydrogenation during the heating stage, we did a series of experiments. From 298 K to 378 K, it needs 40 minutes with the heating rate of 2 K/min. Therefore, we collected and analyzed the mixtures at 10.0 min, 20.0 min and 40.0 min when the reactor is heated, and the results are shown in the following table. It can find that the FOL yield increased faintly during the heating stage, indicating that the performance of FAL hydrogenation would not be affected basically during the heating stage.

### 3.7 The effect of external diffusion

**Table S7.** Hydrogenation of FAL over Cu/AC-$SO_3H$ catalyst[a]

| Run. no. | Stirring speed (rpm) | FOL yield (%) |
|---|---|---|
| 1 | 400 | 85.1 |
| 2 | 700 | 92.6 |
| 3 | 1000 | >99.9 |
| 4 | 1300 | >99.9 |

[a] Reaction conditions: catalyst to FAL mass ratio =1:1, FAL = 1.0 mmol, reaction temperature = 378 K, $H_2$ pressure = 0.4 MPa, reaction time = 120 min, 2-propanol = 5 mL.

In this work, the stirring speed was about 1000 rpm.

### 3.8 Thermodynamic calculation under reaction conditions

**Table S8.** Thermodynamic calculation under the condition of $H_2$ hydrogenation

| Conditions | ΔH (kJ/mol) | ΔS (J/mol/K) | ΔG (kJ/mol) |
|---|---|---|---|
| **$Cu_2O+H_2 \rightarrow 2Cu+H_2O$** | | | |
| $T^{\theta}$=298 K,$P^{\theta}$=1 atm | $\Delta r^{\theta}Hm$= -119.15 | $\Delta r^{\theta}Sm$=-94.85 | $\Delta r^{\theta}Gm$=-90.83 |
| T=378 K, P=4 atm | ΔrHm= -117.11 | ΔrSm=-88.79 | ΔrGm=-83.53 |
| **$CuO+H_2 \rightarrow Cu+H_2O$** | | | |
| $T^{\theta}$=298 K,$P^{\theta}$=1 atm | $\Delta r^{\theta}Hm$= -130.64 | $\Delta r^{\theta}Sm$=-70.86 | $\Delta r^{\theta}Gm$=-109.99 |
| T=378 K, P=4 atm | ΔrHm= -128.52 | ΔrSm=-64.55 | ΔrGm=-104.11 |

ΔrGm<0, it is possible to take place these reduction reactions

**Table S9.**Thermodynamic calculation under the condition of transfer hydrogenation

| Conditions | ΔH (kJ/mol) | ΔS (J/mol/K) | ΔG (kJ/mol) |
|---|---|---|---|
| **$Cu_2O+CH_3\text{-}CH_2(OH)\text{-}CH_3 \rightarrow 2Cu+ CH_3\text{-}CH(O)\text{-}CH_3+H_2O$** | | | |
| $T^{\theta}$=298 K,$P^{\theta}$=1 atm | $\Delta r^{\theta}Hm$= -49.5 | $\Delta r^{\theta}Sm$=54.4 | $\Delta r^{\theta}Gm$=-65.7 |
| T=423 K, P=40 atm | ΔrHm= -46.3 | ΔrSm=62.8 | ΔrGm=-72.9 |
| **$CuO+CH_3\text{-}CH_2(OH)\text{-}CH_3 \rightarrow Cu+ CH_3\text{-}CH(O)\text{-}CH_3+H_2O$** | | | |
| $T^{\theta}$=298 K,$P^{\theta}$=1 atm | $\Delta r^{\theta}Hm$= -60.9 | $\Delta r^{\theta}Sm$=78.4 | $\Delta r^{\theta}Gm$=-84.3 |
| T=423 K, P=40 atm | ΔrHm= -57.5 | ΔrSm=87.3 | ΔrGm=-94.7 |

ΔrGm<0, it is possible to take place these reduction reactions

### 3.9 Comparing between fresh and spent catalyst

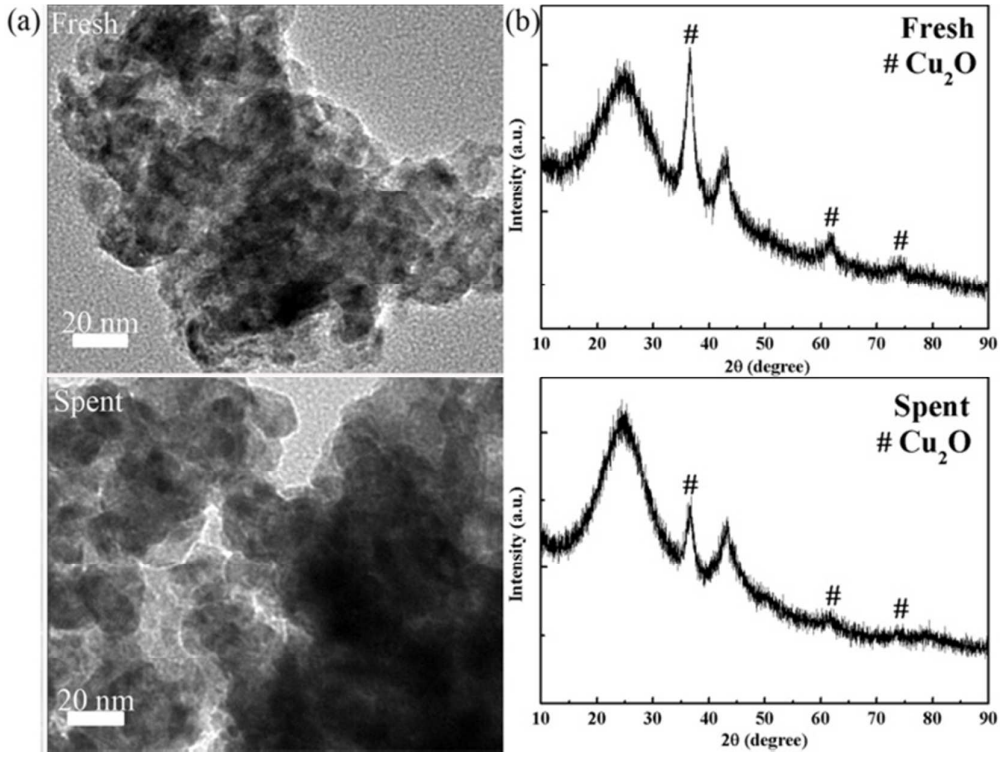


**Figure S7**. (a) Typical TEM images and (b) XRD patterns of Cu/AC-$SO_3H$ (fresh and spent).

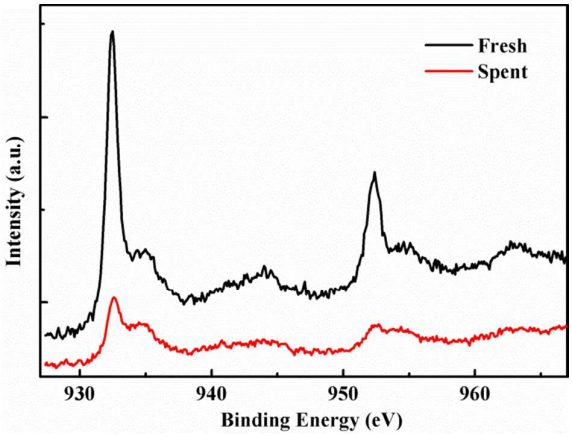


**Figure S8**. Typical XPS patterns of Cu/AC-$SO_3H$ (fresh and spent).

GC data of representative samples

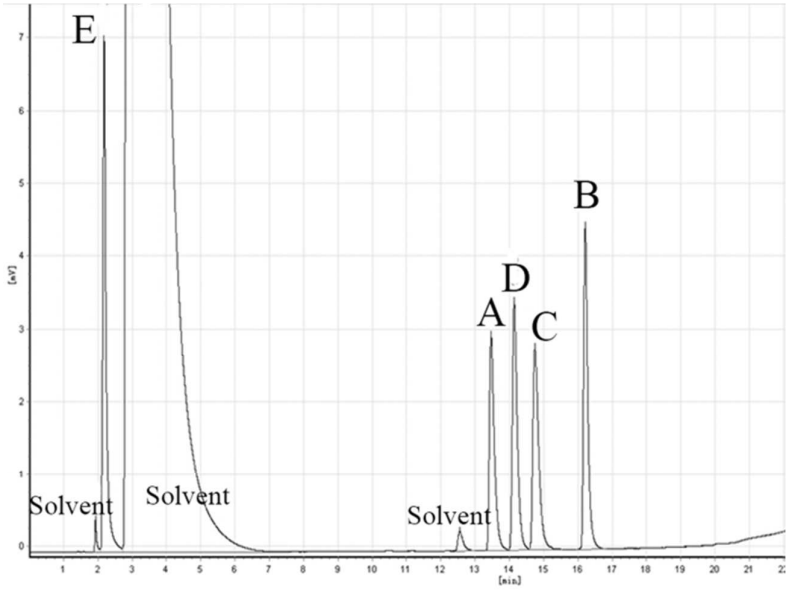


**Figure S9.** Raw GC data of standard samples.

(**A**: furfural; **B**: furfuryl alcohol; **C**: n-octanol; **D**: tetrahydrofurfuryl alcohol; **E**: 2-methyl furan.)

| Peaks for | Retention time | Peak area | Height |
|---|---|---|---|
| **A** | 13.468 | 29978 | 2959 |
| **B** | 16.211 | 38398 | 4445 |
| **C** | 14.745 | 33294 | 2789 |
| **D** | 14.142 | 33916 | 3414 |
| **E** | 2.179 | 46974 | 7040 |

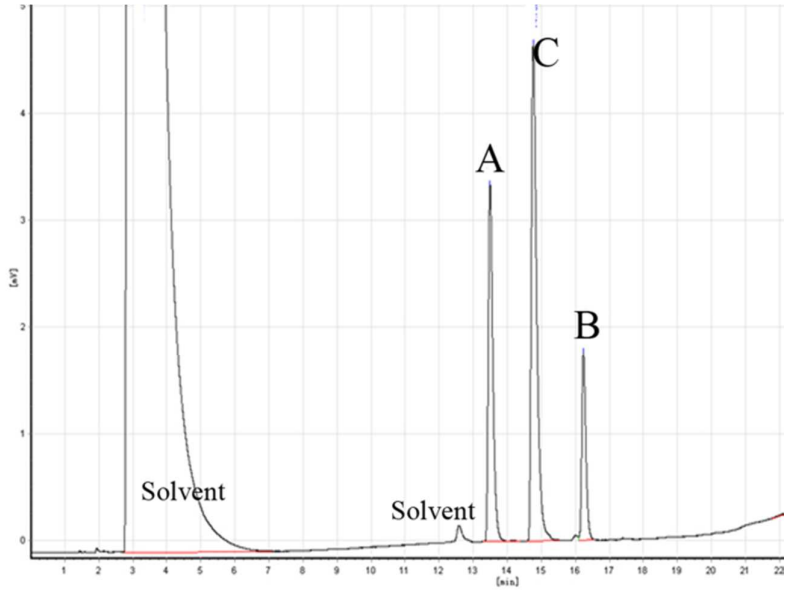


**Figure S10.** Raw GC data for hydrogenation of furfural (**A**) by the supported Cu/AC-$SO_3H$.

(Reaction conditions: catalyst to FAL mass ratio = 1:1; reaction temperature = 368 K; $H_2$ pressure = 0.4 MPa; 2-propanol = 5 mL; reaction time = 180 min)**.**

(**A**: furfural; **B**: furfuryl alcohol; **C**: n-octanol.)

| Peaks for | Retention time | Peak area | Height |
|---|---|---|---|
| **A** | 13.496 | 31269 | 3330 |
| **B** | 16.238 | 14541 | 1756 |
| **C** | 14.762 | 51255 | 4644 |

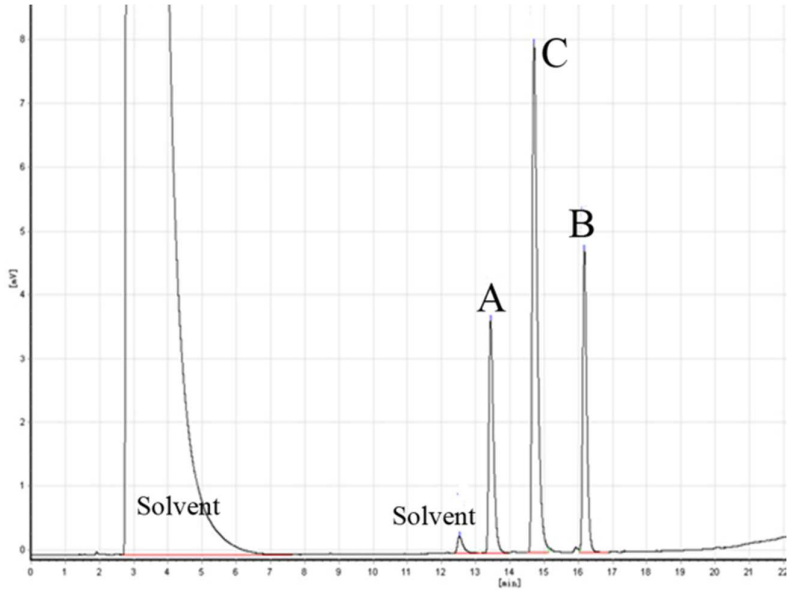


**Figure S11.** Raw GC data for hydrogenation of furfural (**A**) by the supported Cu/AC-$SO_3H$.

(Reaction conditions: catalyst to FAL mass ratio = 1:1; reaction temperature = 373 K; $H_2$ pressure = 0.4 MPa; 2-propanol = 5 mL; reaction time = 180 min)**.**

(**A**: furfural; **B**: furfuryl alcohol; **C**: n-octanol.)

| Peaks for | Retention time | Peak area | Height |
|---|---|---|---|
| **A** | 13.435 | 34466 | 3671 |
| **B** | 16.175 | 39037 | 4745 |
| **C** | 14.704 | 83624 | 7981 |

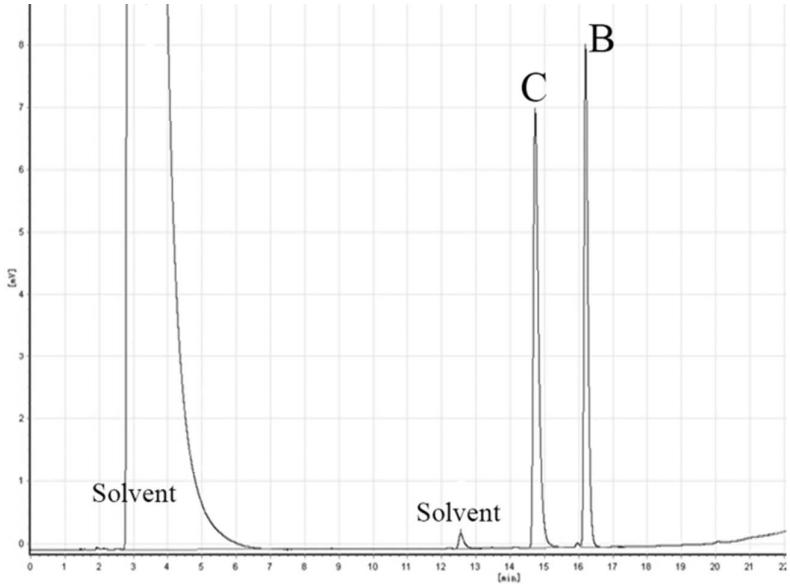


**Figure S12.** Raw GC data for hydrogenation of furfural (**A**) by the supported Cu/AC-$SO_3H$.

(Reaction conditions: catalyst to FAL mass ratio = 1:1; reaction temperature = 378 K; $H_2$ pressure = 0.4 MPa; 2-propanol = 5 mL; reaction time = 120 min)**.**

(**A**: furfural; **B**: furfuryl alcohol; **C**: n-octanol.)

| Peaks for | Retention time | Peak area | Height |
|---|---|---|---|
| **A** | 0.0 | 0 | 0 |
| **B** | 16.203 | 64704 | 7990 |
| **C** | 14.731 | 74541 | 6982 |

(1) Villaverde, M. M.; Bertero, N. M.; Garetto, T. F.; Marchi, A. J. Selective liquid-phase hydrogenation of furfural to furfuryl alcohol over Cu-based catalysts. *Catal. Today* **2013**, *213*, 87-92.

(2) Fulajtarova, K.; Sotak, T.; Hronec, M.; Vavra, I.; Dobrocka, E.; Omastova, M. Aqueous phase hydrogenation of furfural to furfuryl alcohol over Pd-Cu catalysts. *Appl. Catal., A* **2015**, *502*, 78-85.

(3) Vargas-Hernández, D.; Rubio-Caballero, J. M.; Santamaría-González, J.; Moreno-Tost, R.; Mérida-Robles, J. M.; Pérez-Cruz, M. A.; Jiménez-López, A.; Hernández-Huesca, R.; Maireles-Torres, P. Furfuryl alcohol from furfural hydrogenation over copper supported on SBA-15 silica catalysts. *J. Mol. Catal. A: Chem.* **2014**, *383-384*, 106-113.

(4) Villaverde, M. M.; Garetto, T. F.; Marchi, A. J. Liquid-phase transfer hydrogenation of furfural to furfuryl alcohol on Cu-Mg-Al catalysts. *Catal. Commun.* **2015**, *58*, 6-10.

(5) Nagaraja, B. M.; Padmasri, A. H.; David Raju, B.; Rama Rao, K. S. Vapor phase selective hydrogenation of furfural to furfuryl alcohol over Cu–MgO coprecipitated catalysts. *J. Mol. Catal. A: Chem.* **2007**, *265 (1-2)*, 90-97.

(6) Scholz, D.; Aellig, C.; Hermans, I. Catalytic transfer hydrogenation/hydrogenolysis for reductive upgrading of furfural and 5-(hydroxymethyl)furfural. *ChemSusChem* **2014**, *7 (1)*, 268-75.

(7) Dong, F.; Zhu, Y.; Zheng, H.; Zhu, Y.; Li, X.; Li, Y. Cr-free Cu-catalysts for the selective hydrogenation of biomass-derived furfural to 2-methylfuran: The synergistic

effect of metal and acid sites. *J. Mol. Catal. A: Chem.* **2015**, *398*, 140-148.

(8) Mizugaki, T.; Yamakawa, T.; Nagatsu, Y.; Maeno, Z.; Mitsudome, T.; Jitsukawa, K.; Kaneda, K. Direct Transformation of Furfural to 1,2-Pentanediol Using a Hydrotalcite-Supported Platinum Nanoparticle Catalyst. *ACS. Sustain. Chem. Eng.* **2014**, *2 (10)*, 2243-2247.

(9) Sharma, R. V.; Das, U.; Sammynaiken, R.; Dalai, A. K. Liquid phase chemo-selective catalytic hydrogenation of furfural to furfuryl alcohol. *Appl. Catal., A* **2013**, *454*, 127-136.

(10) Srivastava, S.; Mohanty, P.; Parikh, J. K.; Dalai, A. K.; Amritphale, S. S.; Khare, A. K. Cr-free Co–Cu/SBA-15 catalysts for hydrogenation of biomass-derived α-, β-unsaturated aldehyde to alcohol. *Chin. J. Catal.* **2015**, *36 (7)*, 933-942.

(11) Srivastava, S.; Solanki, N.; Mohanty, P.; Shah, K. A.; Parikh, J. K.; Dalai, A. K. Optimization and Kinetic Studies on Hydrogenation of Furfural to Furfuryl Alcohol over SBA-15 Supported Bimetallic Copper–Cobalt Catalyst. *Catal. Lett.* **2015**, *145 (3)*, 816-823.

(12) Merlo, A. B.; Vetere, V.; Ruggera, J. F.; Casella, M. L. Bimetallic PtSn catalyst for the selective hydrogenation of furfural to furfuryl alcohol in liquid-phase. *Catal. Commun.* **2009**, *10 (13)*, 1665-1669.